Pergamon

Acta mater. 49 (2001) 1987–1992

Acta MATERIALIA

www.elsevier.com/locate/actamat

HIGH-TEMPERATURE SUPERCONDUCTOR MATERIALS FOR CONTACT LAYERS IN SOLID OXIDE FUEL CELLS: II. CHEMICAL PROPERTIES AT OPERATING TEMPERATURES

I. ARUL RAJ[1], F. TIETZ[2]†, A. GUPTA[2], W. JUNGEN[2] and D. STÖVER[2]

[1]Central Electrochemical Research Institute, Karaikudi 630 006, Tamil Nadu, India and [2]Institute for Materials and Processes in Energy Systems (IWV-1), Forschungzentrum Jülich, D-52425 Jülich, Germany

(Received 18 January 2001; accepted 20 February 2001)

Abstract—The chemical reactivity between superconducting ceramic materials ($YBa_2Cu_3O_{7-x}$, $Bi_2Sr_2CaCu_2O_{8+x}$ and $Bi_2Sr_2CuO_{6+x}$) and the cathode material of solid oxide fuel cells ($La_{0.65}Sr_{0.3}MnO_3$) was investigated by long-term annealing experiments of pressed powder mixtures lasting two weeks at 850°C. The chemical properties at the operating temperature of a solid oxide fuel cell revealed that all three superconducting materials reacted with $La_{0.65}Sr_{0.3}MnO_3$ and underwent changes in volume and density after annealing. The chemical compatibility between the superconductors and interconnect material, a ferritic steel (X 10 CrAl 18), was investigated using screen-printed thick layers of $Bi_2Sr_2CuO_{6+x}$ on steel substrates. The formation of undesirable products, especially $SrCrO_4$, due to diffusion processes across the interface was confirmed by investigations of metallographic cross-sections. Efforts to stop the interfacial reaction by introducing a thin CuO barrier layer between the superconductor and steel did not solve the problem.

Keywords: Superconductors; Steels; Chemical; Corrosion; Solid oxide fuel cells

I. INTRODUCTION

The development of solid oxide fuel cell (SOFC) technology for electricity production from carbonaceous fuels with reduced pollution has been one of the central topics of research in recent years [1–9]. In the view of the inherent problems of the high-temperature operation conditions of SOFCs at around 1000°C, currently, several groups are concentrating on the development and demonstration of SOFC systems operating in the intermediate temperature range, 650–800°C (IT-SOFC) [1, 3, 6, 10–14] with alternative functional materials and components. Significant results have been reported for IT-SOFC units by various groups [11, 14–21]. The aim of operating an IT-SOFC not only requires more efficient electrocatalysts and better ionic conductive ceramic membranes but also different materials for sealings and electrical contacts between the cells and the interconnecting metallic plates. Therefore materials which soften in the IT-SOFC operation temperature regime, e.g. low-melting ceramics, were considered as a class of materials for such applications. High-temperature superconductors (HTSC) have melting points close to the SOFCs' operation temperature and were investigated in more detail with respect to sintering behavior, electrical conductivity and thermal expansion as possible contact layer materials [22]. As a continuation of this work, the experimental results obtained with respect to the chemical compatibility of the superconductor materials $Bi_2Sr_2CaCu_2O_{8+x}$ (BSCC-2212), $Bi_2Sr_2CuO_{6+x}$ (BSCC-2201) and $YBa_2Cu_3O_{7-x}$ (YBCO) with the adjacent SOFC components, the cathode of the composition $La_{0.65}Sr_{0.3}MnO_3$ (LSM) and the interconnecting metallic plates made of ferritic steel (X 10 CrAl 18) are presented in this paper.

II. EXPERIMENTAL

BSCC-2212 and BSCC-2201 were synthesized by the solid state reaction as well as the citrate complexation reaction as described in detail in Refs. [22, 23]. The powders obtained were subjected to calcination at 800°C for 24 h in air and were ground well prior to further measurements. The LSM powder was synthesized by the spray pyrolysis technique [24], calcined at 900°C and milled in ethanol using a planetary ball mill. For the investigations with $YBa_2Cu_3O_{7-x}$, commercial powder was supplied by

† To whom all correspondence should be addressed. Tel.: +49-2461-615-007; Fax: +49-2461-612-455.
E-mail address: f.tietz@fz-juelich.de (F. Tietz)

1359-6454/01/$20.00
PII: S1359-6454(01)00111-2

Solvay Barium Strontium GmbH, Germany. The ferritic steel was provided by KTN, Germany.

For the investigations of the chemical reactivity of the HTSC powders with LSM, the respective HTSC powder and LSM powder were mixed in a 1:1 weight ratio and ball milled to achieve homogenization. Circular pellets (8 mm in diameter and 4–5 mm in height) were uniaxially pressed at 300 MPa from the above powder mixtures and exposed in air at 800°C for two weeks. The annealed pellets were crushed into powder and subjected to X-ray diffraction (XRD) measurements using a Siemens D 5000 diffractometer.

For the compatibility experiments with the interconnect steel, screen-printing pastes were prepared from the superconductor powders using ethyl cellulose as binder and terpineol as solvent after thorough homogenization on a three-roll mill. The pastes were printed in stripes with a thickness of about 150–250 μm on freshly polished surfaces of ferritic steel plates using a screen printer (model 2400, Mitani). These samples were heat treated at 850°C for 2 h to simulate the assembling process of an SOFC stack. The thickness of the screen-printed layers was measured in using a Dektac II (Sloan Technology Corp.) before and after annealing. Surfaces and polished cross-sections of the annealed samples were investigated by a scanning electron microscope (SEM; LEO 440) equipped with a detector for energy-dispersive X-ray analysis (EDX).

III. RESULTS AND DISCUSSION

A. Reactivity with LSM

The changes measured in the volume as well as density of the LSM/HTSC pellets after continuous annealing at 800°C for two weeks are presented in Table 1. All three samples underwent significant but varying degrees of dimensional changes, which could be ascribed to the distinct but severe thermo-chemical reactivity with LSM because sintering effects could be neglected [22].

The phases obtained in the pellets during annealing by powder XRD are presented in Fig. 1. A new crystalline phase containing lanthanum, namely $Bi_2Sr_{1.7}La_{0.3}CuO_{6.28}$ (JCPDS code 45-0313) [25], was formed during annealing with the bismuth cuprates. The BSCC-2201 was almost completely converted into the new phase whereas a small amount of the original BSCC-2212 phase remained after exposure.

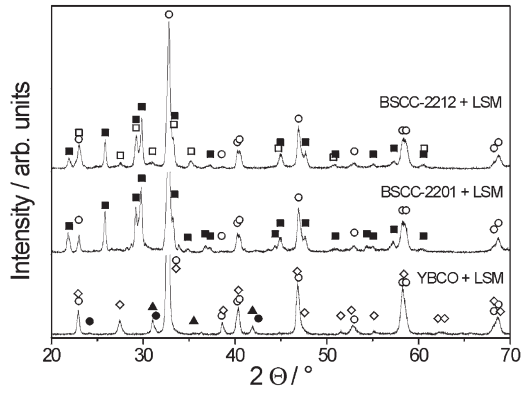

Fig. 1. XRD patterns of the LSM/HTSC powder mixtures after two weeks exposure at 800°C. Besides the superconducting phases BSCC-2212 (□) and YBCO (◇) and the LSM cathode with perovskite structure (○), new phases appear corresponding to the chemical formulae $Bi_2Sr_{1.7}La_{0.3}CuO_{6.28}$ (■), La_2CuO_4 (▲) and $CuCO_3$ (●) [25].

The LSM/YBCO mixture led to the formation of small quantities of a K_2NiF_4-type compound and also of $CuCO_3$. Although the chemical reactivity between LSM and $YBa_2Cu_3O_{7-x}$ was rather slow at 800°C, an additional experiment with a pellet heat treated at 900°C for 2 h gave significant amounts of the K_2NiF_4-type compound, presumably composed of "$(Y,La)_{2-x}(Ba,Sr)_xCuO_4$".

The data on volume expansion indicated that BSCC-2212 expanded more (8.86%) than BSCC-2201 (4.23%). Similarly, the changes observed in the density values also indicated that BSCC-2212 and BSCC-2201 reacted strongly with LSM. The measured values, however, are not a direct measure of the chemical reactivity with LSM because the new phase formed has a very similar chemical composition such as BSCC-2201 and smaller effects on volume and density can be expected. In any case, the reaction with LSM is a drawback of these materials for their eventual application as contact layers in SOFC.

B. Reactivity with ferritic steel

The compositions of the screen-printing pastes are listed in Table 2. The adhesion between the ferritic steel and the HTSC screen-printed layers was very good.

The formation of a yellowish-green reaction product was noticed between steel and BSCC-2201 layer after 2 h at 850°C in air. From a metallographic cross-section the thickness of the reaction zone was determ-

Table 1. Dimensional changes observed on LSM/HTSC pellets (50:50 wt.%) after continuous annealing at 800°C for two weeks in air

Composition	Volume (cm^3)			Density ($g\ cm^{-3}$)		
	Before annealing	After annealing	Change (%)	Before annealing	After annealing	Change (%)
LSM+BSCC-2212	0.2392	0.2604	+8.86	4.019	3.492	−13.11
LSM+BSCC-2201	0.2466	0.2575	+4.23	3.988	3.789	−4.98
LSM+YBCO	0.2779	0.2743	−1.29	3.656	3.545	−3.03

Table 2. Compositions of screen-printing pastes used for the compatibility studies with ferritic steel

Material	Amount of powder (wt.%)	Amount of binder solution[a] (wt.%)	Total amount of solvent (wt.%)
BSCC-2201	78.5	0.7	20.7
YBCO	73.9	0.7	25.4
CuO	61.4	0.5	38.1

[a] Solution of solvent with 10 wt.% binder dissolved.

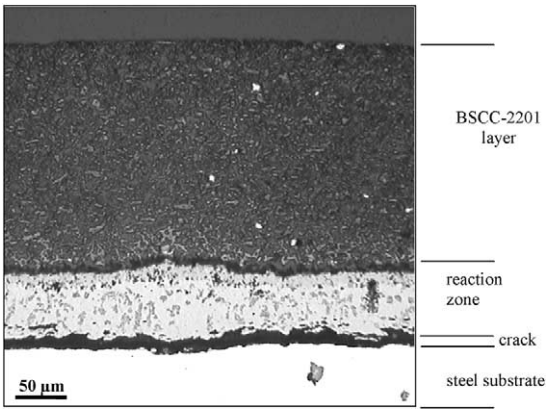

Fig. 2. Optical microscopy image of the reaction zone between BSCC-2201 and ferritic steel after 2 h at 850°C.

ined (about 60 µm, Fig. 2) containing at least three layers with different compositions as indicated by EDX point analysis and element mapping (Fig. 3). The crack between the steel substrate and the oxide scale was induced during metallographic sample preparation.

The reaction zone was found to contain mainly Fe, Cr, and Sr. The top layer of the reaction zone (upper black region in Fig. 2) contained only Sr and Cr and was later identified in an XRD measurement on the sample shown in Fig. 4 as $SrCrO_4$. From the element mapping a pronounced diffusion profile was detected for Cr (Fig. 3), whereas the iron remained in the steel. Therefore the reaction zone can be regarded as a previous part of the steel. Due to the instable interface and continuous release of Cr into the superconductor layer, the cuprate decomposes and the Sr reacts with the Cr to form $SrCrO_4$. Furthermore, the decreased Cr content in the steel surface destabilizes the oxidation resistance of the steel and therefore a thick layer of about 50 µm of $(Fe,Cr)O_x$ was formed below the Sr-rich oxide layers.

After 24 h annealing at 850°C, the BSCC coating had a yellow color and was detached from the substrate (Fig. 4). The interactions with the steel change completely when the exposure temperature is lowered by 50°C. Figure 5 is an optical microscopy image and shows the results of the exposure of $Bi_2Sr_2CuO_{6+x}$ on the steel substrate after 144 h at 800°C. In the surface of the steel substrate deep holes were corroded permitting the growth of large columns of up to 2 mm in length composed of Fe and Cr oxides. Also, the BSCC coating was completely decomposed and separated from the steel interface. Large cavities were formed between the grown columns (Fig. 5).

In order to prevent the reaction between BSCC and the Cr released from the steel, about 5 µm thick CuO layers were printed onto the steel substrates before the cuprate was deposited. Annealing at 850°C for 2 h resulted in good adhesion between the layers and the steel. However, the CuO layers did not sufficiently protect the ceramic from decomposition and very similar interactions as shown in Figs 2 and 3 were observed. These results indicated that Cr diffuses very rapidly across the CuO barrier forming preferentially alkaline earth chromates.

The reaction between YBCO with steel is slower,

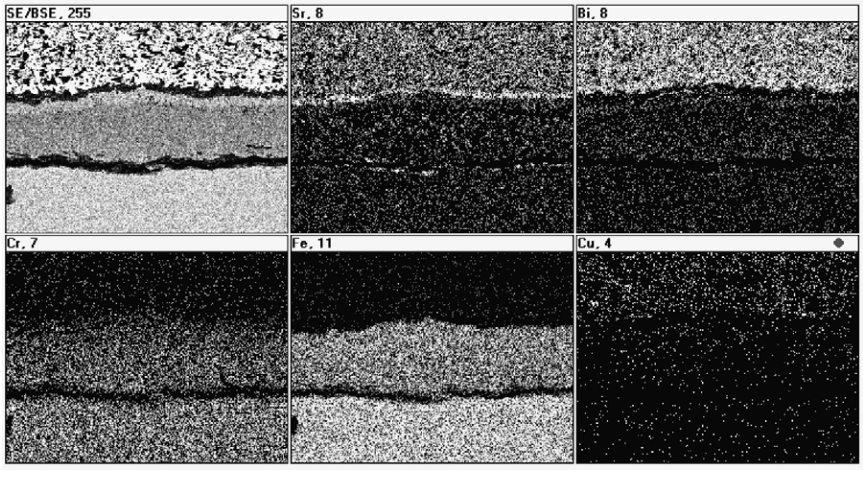

Fig. 3. SEM back-scattering image and element maps of the reaction zone between BSCC-2201 and ferritic steel after 2 h at 850°C (cf. Fig. 2).

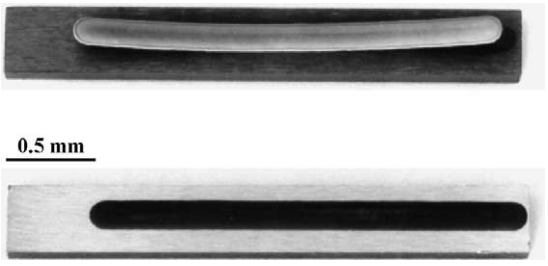

Fig. 4. BSCC layers on ferritic steel substrates before (bottom) and after (top) exposure at 850°C for 24 h.

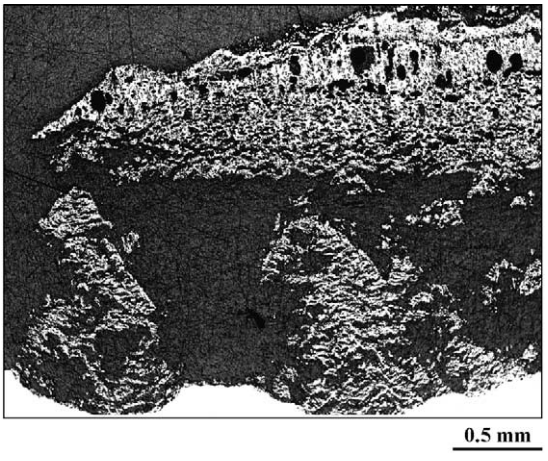

Fig. 5. Polished cross-section of a $Bi_2Sr_2CuO_{6+x}$–steel sample heat treated at 800°C for 144 h. From the steel substrate (white, bottom), large 1.5 mm high columns grew, elevated and decomposed the ceramic coating (top) and created large cavities.

no significant reaction zone was observed after annealing at 850°C for 2 h. However, after 200 h annealing at 800°C this material combination also exhibited fatal corrosion with several layers between the steel and the ceramic (Fig. 6). In this case also the chromium from the steel is the most diffusive species and could be detected deep within the superconductor material. A similar detrimental metal–HTSC interaction was observed after firing, when Ni–Cr (Nichrome), Cr–Al–Co (Kanthal) or Ni–Mo–Fe–Mn (Hastelloy) was used as a core metal for fibre fabrication [26]. Several point analyses by EDX were carried out along the reaction zone (see Fig. 7) to get an impression of the composition of the formed layers and to understand the corrosion process in more detail.

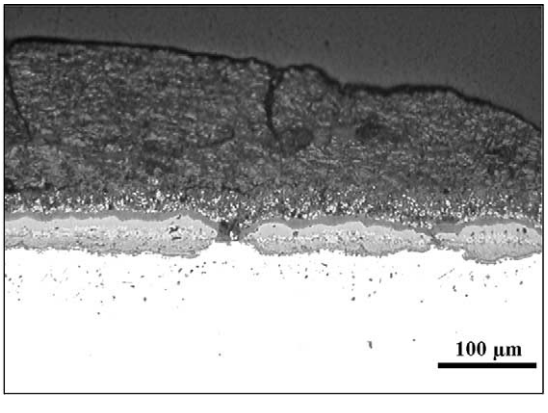

Fig. 6. Polished cross-section of a $YBa_2Cu_3O_{7-x}$–steel sample heat treated at 800°C for 200 h. White, steel substrate; light gray, reaction zone; gray, $YBa_2Cu_3O_{7-x}$.

Table 3. Analytical EDX results of the regions shown in Fig. 7

Point	Analytical result
1	Fe 17.7Cr 1.3Si 0.5Al[a]
2	Fe 14.7Cr 0.98Si[a]
3	$Fe_{0.43}Cr_{0.29}Cu_{0.15}Si_{0.10}Al_{0.03}O_x$[b]
4	$Fe_{0.71}Cr_{0.01}Cu_{0.26}Ba_{0.013}O_x$[b]
5	$Fe_{0.61}Ba_{0.34}Al_{0.05}O_x$[b]$\equiv Ba_{1.02}(Fe_{1.83}Al_{0.15})O_4$
6	$Ba_{0.44}Cr_{0.40}Cu_{0.16}O_x$[b]

[a] Values of alloyed elements in wt.%.
[b] Normalized to 1 mol of cations per formula unit.

The analysis of point 1 gave the initial composition of the steel. Near the surface where no Fe-rich oxide scales are formed the Cr content of the alloy is greatly reduced. This Cr is diffused into the ceramic and is detected at the densified region above (point 6). The thick oxide scales next to point 2 contain mainly Fe oxide, but also significant amounts of Cr, Cu and Si. However, the content of Cr is much lower than at point 6. The outer corrosion scale (point 5) is only composed of Fe, Ba and small amounts of Al.

The degradation of the superconductor material starts with the fast diffusion of chromium species into the ceramics. Even near the outer surface of the $YBa_2Cu_3O_{7-x}$ coating, i.e. about 200 µm from the steel–HTSC interface (Fig. 6), significant concentrations of Cr were detected. When the impurity level exceeds a critical value, not only do the physical properties deteriorate, as is known from several studies [27, 28], but additional phases such as Y_2BaCuO_5, $BaCuO_2$ and K_2NiF_4-analogue compounds containing the transition metals of the steel are also formed [28].

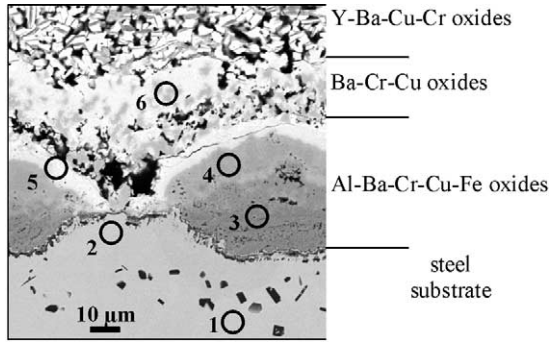

Fig. 7. SEM picture in back-scattering mode of the cross-section of the reaction zone between the ferritic steel and $YBa_2Cu_3O_{7-x}$ after 200 h at 800°C (detail of Fig. 6). The circles indicate regions in which EDX analyses were recorded (see Table 3).

The initial stages of the chemical reactions certainly include disruptions of Cu–O bonds and oxygen withdrawal from the cuprates as has been found for the interaction of metallic Fe with $La_{1.85}Sr_{0.15}CuO_4$ [29, 30]. The decomposition products of $YBa_2Cu_3O_{7-x}$ mostly contain less Ba and, generally speaking, the HTSCs can be regarded as a source of alkaline-earth elements reacting with the metal or oxide scales of the steel, either forming a layer of $SrCrO_4$ in the case of the bismuth-containing superconductors (Fig. 2) or ternary Ba–transition metal oxides as shown in Fig. 7 and Table 3 (points 5 and 6) in the case of $YBa_2Cu_3O_{7-x}$.

With respect to SOFC applications, the HTSC materials have to be evaluated on the basis of their sinterability during the assembling procedure as well as their chemical and electrical properties during operation. The shrinkage of $Bi_2Sr_2CaCu_2O_{8+x}$ and $Bi_2Sr_2CuO_{6+x}$ is not beneficial compared to currently used materials. The two materials also do not become soft close to their melting points [22, 31], so that slight pressure could be applied to reduce the gap between the interconnect plates instead of a sinter shrinkage. On the contrary, the results on the screen-printed $YBa_2Cu_3O_{7-x}$ appeared promising and shrinkage up to 20% was obtained [32] together with well-connected HTSC particles. Furthermore, this more compact microstructure is the reason why $YBa_2Cu_3O_{7-x}$ had more than two and five times higher electrical conductivity than $Bi_2Sr_2CaCu_2O_{8+x}$ and $Bi_2Sr_2CuO_{6+x}$, respectively, as reported in the first part of this series of publication [22].

Finally, chemical interaction with ferritic steel is detrimental to all compounds investigated. Although corrosion with $YBa_2Cu_3O_{7-x}$ is less severe than with the Bi cuprates, there are very strong and damaging interactions with the metal which would lead to failure of an SOFC system within several hundreds of hours. In order to use the beneficial sintering behavior of $YBa_2Cu_3O_{7-x}$, an additional corrosion-protection layer is needed to separate the steel–HTSC interface and to reduce the Cr emission from the steel.

IV. CONCLUSIONS

The chemical interaction with the interconnect material is severe and detrimental. After exposure at 800°C, a thick insulating layer of $SrCrO_4$ was formed at the metal–ceramic interface in the case of $Bi_2Sr_2CuO_{6+x}$. A coating of $YBa_2Cu_3O_{7-x}$ contained large amounts of chromium thus decreasing the electrical conductivity and decomposing the HTSC at the interface. The application of HTSC materials is therefore only possible if protective coatings are deposited on the steel to prevent Cr release from the interconnect.

Acknowledgements—The authors thank M. Kappertz (FZJ—IWV-1) R. Fisseler and E. Wessel (FZJ—IWV-2) for their experimental contributions to this work. Financial support from CSIR, New Delhi, and BMBF-IB-WTZ, Bonn, to carry out this joint research work under the Indo-German bilateral co-operation project (grant no. IND 99/041) is gratefully acknowledged.

REFERENCES

1. Buchkremer, H. P., Diekmann, U., de Haart, L. G. J., Kabs, H., Stimming, U. and Stöver, D., in *Proceedings of the 5th International Symposium on Solid Oxide Fuel Cells (SOFC-V)*, eds. U. Stimming, S. C. Singhal, H. Tagawa and W. Lehnert. The Electrochemical Society, Pennington, NJ, USA, 1997, p. 160.
2. Ishihara, T., Matsuda, H. and Takita, Y., *J. Am. Chem. Soc.*, 1994, **116**, 3801.
3. Feng, M. and Goodenough, J. B., *Eur. J. Solid State Chem.*, 1994, **31**, 663.
4. Ohno, Y., Nagata, S. and Sato, H., *Solid State Ionics*, 1983, **9/10**, 1001.
5. Koe, R. and Anderson, H. U., *J. Mater. Sci.*, 1992, **27**, 5837.
6. Steele, B. C. H., *Solid State Ionics*, 1996, **86–88**, 1223.
7. Aruna, S. T., Muthuraman, M. and Patil, K. C., *Solid State Ionics*, 1998, **111**, 45.
8. Maiti, H. S., Chakraborthy, A. and Paria, M. K., in *Proceedings of the 3rd International Symposium on Solid Oxide Fuel Cells (SOFC-III)*, eds. S. C. Singhal and H. Iwahara. The Electrochemical Society, Pennington, NJ, USA, 1993, p. 190.
9. Iwahara, H., *Solid State Ionics*, 1988, **28–30**, 573.
10. Long, N. J., Lecarpentier, F. and Tuller, H. L., *J. Electroceram.*, 1999, **3**, 399.
11. Bakker, W. T., Huang, K., Goodenough, J. B., Khandkar, A., Elangovan, S. and Milliken, C., *The 1998 Fuel Cell Seminar, Palm Springs, CA, 16–19 November*, 1998, p. 250.
12. Huang, P. and Petric, A., *J. Electrochem. Soc.*, 1996, **143**, 1644.
13. Ishihara, T., Honda, M., Shibayama, T., Minami, H., Nishiguchi, H. and Takita, Y., *J. Electrochem. Soc.*, 1998, **145**, 3177.
14. Stöver, D., Diekmann, U., Flesch, U., Kabs, H., Quadakkers, W. J., Tietz, F. and Vinke, I. C., in *Proceedings of the 6th International Symposium on Solid Oxide Fuel Cells (SOFC-VI)* eds. S.C. Singhal and M. Dokiya. The Electrochemical Society, Pennington, NJ, USA, 1999, p. 812.
15. Tsai, T. and Barnett, A., in *Proceedings of the 5th International Symposium on Solid Oxide Fuel Cells (SOFC-V)*, eds. U. Stimming, S.C. Singhal, H. Tagawa and W. Lehnert. The Electrochemical Society, Pennington, NJ, USA, 1997, p. 369.
16. Maric, R., Ohara, S., Fukui, T., Inagaki, T. and Fujita, J., *Electrochem. – Solid State Lett.*, 1998, **1**, 201.
17. Samson Nesaraj, A., Arul Raj, I. and Pattabiraman, A., in *Proceedings of the 1st Asian Conference on Solid State Ionic Devices, Science and Technology, Chennai, 22–24 March 2000*, ed. S. Chelladurai. p. 108.
18. Ghosh, D., Wang, G., Brule, R., Tang, E. and Huang, P., in *Proceedings of the 6th International Symposium on Solid Oxide Fuel Cells (SOFC-VI)*, eds. S. C. Singhal and M. Dokiya. The Electrochemical Society, Pennington, NJ, USA, 1999, p. 822.
19. Uchida, H., Yoshida, M. and Watanabe, M., *J. Phys. Chem.*, 1995, **99**, 3282.
20. Tsuneyoshi, K. and Sawata, A., *J. Electrochem.Soc.*, 1991, **138**, 1867.
21. Föger, K., Donelson, R. and Ratnaraj, R., in *Proceedings of the 6th International Symposium on Solid Oxide Fuel Cells (SOFC-VI)*, eds. S.C. Singhal and M. Dokiya. The Electrochemical Society, Pennington, NJ, USA, 1999, p. 95.
22. Tietz, F., Arul Raj, I., Jungen, W., Stöver, D., *Acta mater.* 2001, **49**, 803.

23. Pechini, P. M., US Patent No.: 3,330,697, July 11, 1967.
24. Kountouros, P., Förthmann, R., Naoumidis, A., Stochniol, G. and Syskakis, E., *Ionics*, 1995, **1**, 40.
25. International Centre for Diffraction Data, Updated JCPDS Database, Newton Square, PA, 1998.
26. Mizuguchi, J., Suzuki, M., Yamato, H. and Matsumura, M., *J. Electrochem. Soc.*, 1991, **138**, 2942.
27. Zhou, X. Z., Raudsepp, M., Pankhurst, Q. A., Morrish, A. H., Luo, Y. L. and Maartense, I., *Phys. Rev. B*, 1987, **36**, 7230.
28. Tarascon, J. M., Barboux, P., Miceli, P. F., Greene, L. H., Hull, G. W., Eibschutz, M. and Sunshine, S. A., *Phys. Rev. B*, 1988, **37**, 7458.
29. Weaver, J. H., Gao, Y., Wagener, T. J., Flandermeyer, B. and Capone, D. W. II, *Phys. Rev. B*, 1987, **36**, 3975.
30. Hill, D. M., Meyer, H. M. III, Weaver, J. H., Flandermeyer, B. and Capone, D. W. II, *Phys. Rev. B*, 1987, **36**, 3979.
31. Tietz, F., Gupta, A., Jungen, W., Wessel, E., Arul Raj, I. and Stöver, D., in *Proceedings of the 1st International Conference on Advances in Materials Processing, Rotorua, New Zealand, November 2000*, eds. D. L. Zhang, K. L. Pickering and X. Y. Xiong. Institute of Materials Engineering Australasia Ltd., 2000, p. 385.
32. Tietz, F., Gupta, A., Wessel, E. and Arul Raj, I., *Proceedings of the Materials Week 2000, Munich, Germany, October*, 2000, (in press).